J Mol Model (2013) 19:3551–3568
DOI 10.1007/s00894-013-1867-z

ORIGINAL PAPER

A new theoretical analysis of the cooperative effect in T-shaped hydrogen complexes of $C_nH_m\cdots HCN\cdots HW$ with n=2, m=2 or 4, and W=F or CN

Boaz G. Oliveira · Tamires F. Costa · Regiane C. M. U. Araújo

Received: 1 February 2013 / Accepted: 23 April 2013 / Published online: 31 May 2013
© Springer-Verlag Berlin Heidelberg 2013

Abstract In this theoretical work, a new idea about cooperativity in intermolecular clusters of $C_nH_m\cdots HCN\cdots HW$ stabilized by hydrogen bonds composed by lone-electron pairs (nitrogen) and π clouds (C=C and C≡C) as proton acceptors is developed. The structural study and vibrational analysis have pointed out deformations in the intermolecular clusters caused by the HW terminal proton-donor, in which if W=fluorine the largest perturbation occurs. On the contrary, the HCN molecule is considered an intermolecular mediator because its structure is practically unaltered upon the formation of the trimolecular complexes. In order to understand the real contribution of the proton-donor either mediator (HCN) or terminal (HW with W=CN or F), a chemometric analysis was performed uniquely to discover which interaction plays a key role in the collapse of the cooperative effect. The formation of strongest interactions leads to more drastic variations in the energy distribution. In this way, the application of the quantum theory of atoms in molecules (QTAIM) has been extremely important because the hydrogen bond strengths followed by indiciums of covalence were predicted, and therefore the cooperative effect could be understood at last.

Keywords Cooperative effect · DFT · Hydrogen bond · PCA · QTAIM

Electronic supplementary material The online version of this article (doi:10.1007/s00894-013-1867-z) contains supplementary material, which is available to authorized users.

B. G. Oliveira (✉)
Instituto de Ciências Ambientais e Desenvolvimento Sustentável, Universidade Federal da Bahia, 47801-100 Barreiras, Brazil
e-mail: boazgaldino@gmail.com

T. F. Costa · R. C. M. U. Araújo
Departamento de Química, Universidade Federal da Paraíba, 58036-300 João Pessoa, PB, Brazil

Introduction

Some years ago the universe of the noncovalent contacts evolved and nowadays is considered widely diversified owing to a immense variety of molecular interactions [1–3], e.g., van der Waals or London dispersion forces [4], π-stacking in sandwich configurations [5], dihydrogen bonds [6], and as well as the centennial hydrogen bond [7]. As it is well-known, the hydrogen bond [8] consecrated itself as one of the pillars in the evolution of the contemporary science [9] with applications in the fields of chemistry [10, 11], physics [12], and biology [13]. In addition to this, Wilson [14] has defended the importance of the hydrogen bond and its applicability into an area denominated as supramolecular chemistry [15–17]. By definition, supramolecular chemistry discerns a large molecular system as a whole instead of small isolated entities, although these individual subunits contribute decisively to the organization of the ensemble through the balance of intermolecular forces typical of hydrogen bonds [18].

As advocated by Shi et al. [19], Müller et al. [20], as well as Borho and Suhm [21], not always is the supramolecular organization represented by macromolecular systems [22]. Actually, the ratiocination and interpretation of the supramolecular chemistry properties are equivalent to those used for studying small or medium aggregates, which are currently named as clusters [23]. In this last one, the chemical literature disposes a large number of works, in general some of them reveal that monoprotic acids such as HF [24], HCl [25], HCN [26], or even cations and anions [27, 28] can

form a supramolecular system. As such, the aim of these investigations is routinely concentrated in the measurement of the non-additivity (NA) or cooperative energy (CE) [29], a resulting effect from stable hydrogen bonds consecutively aligned between each individual molecular block [30, 31]. In other words, CE translates the energy distribution as well as the possibility for polarization effects to arise [32, 33], whose intensities are completely governed by the hydrogen bond strengths, by which the chemical key for understanding the stabilization of the molecular cluster can be unveiled.

At this current time, the quantification of CE is routinely performed on small homoclusters composed by identical monomeric units [24–26, 34, 35]. Ideally, it is worthwhile to demonstrate that the energy distribution is equally dispersed among all hydrogen bonds and thereby their strengths are of nearly equal magnitude. In the articles signed by Parra [36], Canuto [37], Chen [38], Yeole and Gadre [39], they affirm that CE can be interpreted by means of algebraic formulations, by which all electronic distortions are computed in order that CE can be carefully predicted. However, our purpose is not the evaluation of CE in homoclusters [40], quite the opposite heteroclusters are our investigating systems [41], in the same way to those examined by Grabowski and Leszczynski [42]. Actually, this insight converges to two basic questions: *i*) Should the models used to interpret CE in homoclusters also be efficient when applied to heteroclusters? *ii*) By considering the level of theory, e.g., some DFT hybrid or any MBPT method, how the energy distribution (properly the hydrogen bond energies) and molecular polarity (in this case caused by charge transference or electronic density) influence in the measurement of CE? As has been examined by Song et al. [43], among a series of density-functional approaches B3LYP was classified as accurate for computing the interaction energies as well as predict properties in total synergism with experimental data [44]. Moreover, Nakano et al. [45] have concluded that BHandHLYP is also efficient to be used in cooperative studies of molecular systems [6]. Indeed, the choice of a computational level fitted to capture the dispersion and electronic correlation is one of the most debated questions in theoretical chemistry, but it will be demonstrated later in "Selection of the theoretical levels" that B3LYP and BHandHLYP in association with the 6-311++G(d,p) basis set furnishes efficient theoretical levels, and thereby they were chosen to be used in the study of the C_nH_m···HCN···HW systems.

Because the mainstream upon forming the supermolecule is the interaction strength [46], the practicality of the two inquiries mentioned above is closely dependent on the hydrogen bond framework, i.e., the electronic charge concentration in the protons-acceptor in association with the protons-donor capability of some molecules and, mainly, which atoms or molecular groups should be included in this conception [47]. In a recent paper, Desiraju has grouped a series of characteristics and modern concepts elaborated to recognize the hydrogen bond in any intermolecular system [48]. To reaffirm the importance of this study, it was necessary to account all electronic phenomena of the hydrogen bonding, and thereby the following scheme was established: Z–Y···H–W in which Z and W are centers containing higher electronegative than hydrogen whereas Y is a charge density region formed by lone pairs of electrons [47, 49] or by unsaturated hydrocarbon sites [50, 51], such as the π bonds of acetylene (C_2H_2) or ethylene (C_2H_4) [52, 53]. Regarding these last ones, once they are unusual charge density centers albeit even so operate as proton acceptors, the interaction is aligned toward the middle point of the π bond, except when acetylene is paired with two monoprotic acids [54]. Thereby the geometries of the π complexes C_2H_2···HW and C_2H_4···HW are similar to a T-shape structure [55, 56]. Besides the evaluation of the acetylene capacity to form T-shaped clusters with monoprotic acids, e.g., HF and HCN [57, 58], the great goal of this current work is not concentrated only on describing the structure of the π-n complexes C_2H_2···HCN···HF, C_2H_2···HCN···HCN, C_2H_4···HCN···HF, and C_2H_4···HCN···HCN (π=unsaturated bonds and n=lone-electron pairs) in order to measure the hydrogen bond strength [59], quantification of the charge transfer or even by the analysis of the stretch frequencies of the vibrational harmonic spectrum, but we wish to know whether the models often used to estimate CE changes in homoclusters (xHCN with x=2 or higher, for instance) may be applied in heteroclusters, as already pointed out in this work.

Methodologies

Useful models to describe the cooperative effect

The stabilization energy (ΔE) of heterotrimeric systems obtained through the performance of computational calculations is defined according to the supermolecule approach [60]:

$$\Delta E_{(A\cdots B\cdots C,\ldots)} = E_{(A\cdots B\cdots C,\ldots)} - \sum E_{(A,\,B,\,C,\ldots)} \quad (1)$$

In works elaborated exclusively to study the π hydrogen-bonded complexes [61–63], the calculations of the basis sets superposition error (BSSE) [64, 65] and the quantifications of the zero-point energy (ZPE) are applied compulsorily to correct the values of the stabilization energies. In this sense, the BSSE-corrected H-bond energy (ΔE^C) can be obtained by summing the BSSE amount and the ΔZPE result into the stabilization energy:

$$\Delta E^C = \Delta E + BSSE + \Delta ZPE \quad (2)$$

However, the counterpoise method developed by Boys and Bernardi [66] when applied to heterotrimeric systems (Eq. 3) lead us to assume the extension effect of the basis set from the monomers onto dimers, trimers, and so on.

$$\mathrm{BSSE} = \left[E_{(A)} - E_{(A)}^{A(B\cdots C)ghost}\right] + \left[E_{(B)} - E_{(B)}^{B(A\cdots C)ghost}\right] + \left[E_{(C)} - E_{(C)}^{C(A\cdots B)ghost}\right] \quad (3)$$

For instance, the molecular orbitals of B and C should be zero (ghost) while the generalized term $E_{(A)}^{A(B\cdots C)ghost}$ account for the energy of the monomer A within the A···B···C heterotrimer. By this insight, Wells and Wilson [67] have created a scheme named site-site function counterpoise (SSFC) in which the ghost energies within the cluster are quantified as follows:

$$\Delta E^{CP}_{(A\cdots B\cdots C)} = E_{(A\cdots B\cdots C)} + \left[E_{(A)} - E_{(A)}^{(B\cdots C)ghost}\right] + \left[E_{(B)} - E_{(B)}^{(A\cdots C)ghost}\right] + \left[E_{(C)} - E_{(C)}^{(A\cdots B)ghost}\right] \quad (4)$$

If the A···B···C heterotrimer represents the intermolecular model of interest, besides the concurrent $E_{(A\cdots B\cdots C)}$ interaction, the $E_{(A\cdots B)}$, $E_{(B\cdots C)}$, and $E_{(A\cdots C)}$ binary ones also shall be embodied in the analysis of both $\Delta E^{CP}_{(A\cdots B\cdots C)}$ and CE. As such, the elaboration of the Valiron Meyer function counterpoise (VMFC) [68] took into account this insight,

$$\Delta E^{CP}_{(A\cdots B\cdots C)} = E_{(A\cdots B\cdots C)} + \left[E_{(A)} - E_{(A)}^{(B\cdots C)ghost}\right] + \left[E_{(B)} - E_{(B)}^{(A\cdots C)ghost}\right] + \left[E_{(C)} - E_{(C)}^{(A\cdots B)ghost}\right] + \left[E_{(A\cdots B)} - E_{(A\cdots B)}^{(C)ghost}\right] + \left[E_{(B\cdots C)} - E_{(B\cdots C)}^{(A)ghost}\right] + \left[E_{(A\cdots C)} - E_{(A\cdots C)}^{(B)ghost}\right] \quad (5)$$

In a paper elaborated specially to compare these two schemes, Salvador and Szczęśniak [69] have shown that VMFC yields more accurate results or less overestimated corrections. Furthermore, the most unambiguous way to define the counterpoise contribution is the counting of the interaction energies into units of two-bodies (Δ^2) and three-bodies (Δ^3), as proposed by Hankins, Moskowitz, and Stillinger [70]:

$$\Delta^2 E^{CP}_{(A\cdots B)} = E_{(A\cdots B)}^{A\cdots B(C)ghost} - \left[E_{(A)}^{A(B\cdots C)ghost} + E_{(B)}^{B(A\cdots C)ghost}\right] \quad (6)$$

$$\Delta^2 E^{CP}_{(B\cdots C)} = E_{(B\cdots C)}^{B\cdots C(A)ghost} - \left[E_{(B)}^{B(A\cdots C)ghost} + E_{C}^{C(A\cdots B)ghost}\right] \quad (7)$$

$$\Delta^2 E^{CP}_{(A\cdots C)} = E_{(A\cdots C)}^{A\cdots C(B)ghost} - \left[E_{(A)}^{A(B\cdots C)ghost} + E_{(C)}^{C(A\cdots B)ghost}\right] \quad (8)$$

$$\Delta E^{CP}_{(A\cdots B\cdots C)} = \Delta^2 E^{CP}_{(A\cdots B)} + \Delta^2 E^{CP}_{(B\cdots C)} + \Delta^2 E^{CP}_{(A\cdots C)} + \Delta^3 E^{CP}_{(A\cdots B\cdots C)} \quad (9)$$

As we shall see, the total interaction energy is obtained through the sum of the two- and three-bodies interactions, but the contribution $\Delta E^{CP}_{(A\cdots B\cdots C)}$ of the SSFC approach is easily perceived:

$$\Delta^3 E^{CP}_{(A\cdots B\cdots C)} = \Delta E^{CP}_{(A\cdots B\cdots C)} - \Delta^2 E^{CP}_{(A\cdots B)} - \Delta^2 E^{CP}_{(B\cdots C)} - \Delta^2 E^{CP}_{(A\cdots C)} \quad (10)$$

Henceforth, it is important to know whether CE of the π-n C_2H_2···HCN···HF and C_2H_2···HCN···HCN complexes can be estimated by means of the equations demonstrated above. This is one of the greatest aims of this work.

Selection of the theoretical levels

In theoretical chemistry, the parallelism between computational approaches is one of the most traditional comparative procedures in studies of electronic structure. Due to large number of available computational algorithms, the comparison among them is more and more necessary because the accuracy and efficiency among them must be known. For instance, the specific comparison between the capacity of some DFT hybrids and accuracy of *ab initio* methods is a routine procedure in any theoretical analysis, and this can be seen in a series of works [70–74]. Undeniably, there cannot be doubt about the most appropriate theoretical method to study weakly bound systems [75–78], in particular, those formed by hydrogen bonds [79, 80]. Nowadays, there are several criteria that justify the applicability of the DFT on examining the hydrogen bond properties [81], even so we should mention that up to now the most relevant of our interest is the computation of the ΔE and CE in the π-n C_2H_2···HCN···HF and C_2H_2···HCN···HCN complexes. In an investigation of hydrogen bonds on cyclic structures, Maes et al. [82] have shown that B3LYP is well-adjusted to observe the cooperative strength, whose results accord satisfactorily with other available works in the literature [83]. Furthermore, Lin and co-authors [84] have divulged results of interaction energies in sequences of amino-acids, wherein

the BHandHLYP functional was considered the best performer among all DFT methods, and better than MP2 could do reasonably well. Concordant to the reports of Winter et al. [85] and Lovas et al. [86], the efficacy of BHandHLYP in hydrogen bond studies is quite similar to post-Hartree-Fock methods, such as CCSD, for instance. In an analysis 'term-by-term', Guadarrama and co-workers affirmed that B3LYP and BHandHLYP are useful to assess the interaction energies and distances of noncovalent systems stabilized through the formation of hydrogen bonds [87], specifically in carbon chains [88].

Very recently, Xu et al. [89] and Sherril et al. [90] have performed robust tests with a group of DFT hybrids [91] in the purpose to know the real capacity of this theory on describing intermolecular interactions [92]. In regards to the conclusions of these works, both the BHandHLYP and B3LYP were considered excellent approaches, which lead us to consider these hybrids as our standard calculation levels. In association with the 6-311++G(d,p) basis set, the theoretical levels BHandHLYP/6-311++G(d,p) and B3LYP/6-311++G(d,p) and the traditional comparison between them seems to be useful to predict the optimized structures, infrared stretch frequencies as well as the electronic parameters of the π-n C_2H_2···HCN···HF and C_2H_2···HCN···HCN complexes. Besides the SCF energy, the CE evaluation can also be developed at light of topological operators. Among several ones known, the electronic density is one of the most important [93], and it can be theoretically estimated by means of calculations inherent to the Bader's quantum theory of atoms in molecules (QTAIM) [94, 95].

Topological conditions for molecular cooperativity

Since the first theoretical works dedicated to the development of algorithms used to implement specific methods for studying the electronic structure, the QTAIM singularity has been considered one of the most useful methods and its application is routinely decisive in research realized in almost all fields of chemistry [96–98]. Composed by quantum mechanics postulates, physical theories, and elegant mathematical formulations, the QTAIM was conceived in order to capture all phenomenology of the chemical bond and molecular stability [99, 100]. By taking into account that the electronic dynamics is relatively chaotic in molecular sites highly rich in electrons but softly condensed in electronic depletions, the QTAIM capability delineates a mapping of the electronic density over the whole molecular surface [101]. In practice, QTAIM localizes an atomic frontier conditioned by the cooperative exchange of charge density and momentum among all chemical elements, which are so-called as open quantum systems [102]. For Bader and Ngyen-Dang: '…*chemistry is the study of matter at the atomic level*' [103]. Thus, it is quite important to know the molecular boundary, which operates to separate neighboring basins of a closed surface (S) into a space (R^3) as follows:

$$\nabla\rho_{(r)}.\mathbf{n}_{(r)} = 0 \tag{11}$$

Whenever this condition is satisfied, a zero-flux surface along of all molecule is modeled. Henceforth, the second derivative of $\nabla\rho_{(r)}$, namely as Laplacian $\nabla^2\rho_{(r)}$, contains the sum of the eigenvalues of the Hessian Matrix ($\nabla^2\rho_{(r)} \equiv \lambda_1+\lambda_2+\lambda_3$) [104], whereas the electronic density $\rho_{(r)}$ is described as a set of critical points, wherein among them we can cite the bond critical points (BCP) identified between pairing of atoms. It is, thus, through the location of the BCP that the electronic density is computed as well as the Laplacian profiles indicate depletion and concentration of charge density whether $\nabla^2\rho_{(r)}>0$ and $\nabla^2\rho_{(r)}<0$, respectively. The physical idea of this observation is supported by the relationship between the Laplacian and the kinetic and potential operators embodied into the virial theorem of the QTAIM approach [105]. Thus, by the foundations of the QTAIM in particular its description of the atomic cooperativity, we also expect that the topology of the C_2H_2···HCN···HF and C_2H_2···HCN···HCN complexes can be well examined, in a similar way to the works reported by Mosquera et al. [106], Solimannejad et al. [107], and Song et al. [108].

Chemometry for theoretical analysis

Multiple interactions are indispensable for the formation of molecular clusters, wherein the energy dynamism remains condensed in a non-cooperative form. At first sight, no direct formulation seems to be capable to discriminate which is the dominant interaction, although indirectly this can be predicted by means of energy distribution approaches. In this view, it should also be reminded that several studies of electronic structures and related phenomena have been performed successfully on the basis of chemometric techniques, such as the principal component analysis (PCA) [109], for instance. In a very short but needed overview, the PCA protocol converts observations into a new coordinate system with uncorrelated values so-called principal components. This is an orthogonal transformation processed to discriminate information of the maximum variance into fewer number of principal components. Mathematically, if a data matrix X^T is taken into account, a matrix W containing eigenvectors orthogonally aligned to the covariance matrix X^TX is given by Y^T as follows:

$$Y^T = X^TW \tag{12}$$

Each Y^T simply represents a rotation of the corresponding row (samples) of X^T. The columns (variables) of Y^T are

constructed by the score values of the first and second PCA, or subsequent ones, if need be [110].

Computational procedure and calculation details

The optimized geometries of the π-n C_2H_2···HCN···HCN, C_2H_2···HCN···HF, C_2H_4···HCN···HCN, and C_2H_4···HCN···HF complexes were obtained at the B3LYP/6-311++G(d,p) and BHandHLYP/6-311++G(d,p) levels of theory. It should be worthwhile to announce that no imaginary frequency has been observed in infrared spectra analysis, and thereby these complexes were characterized in minima of the potential energy surfaces. In all calculations, the optimized geometries of the complexes and monomers were determined through the calculations executed by both versions 98W [111] and 03W [112] of the GAUSSIAN program. We decided to use the version 98W of the GAUSSIAN program because the BSSE calculations are performed when the 'massage' keyword is activated and its application becomes reliable by the determination of the 'ghost' energy for each monomer within a dimer or trimer. On the contrary, by means of the 'counterpoise=n' keyword (where n=2, 3, and 4 represent respectively the dimer, trimer, tetramer, and so on) implemented in the version 03W of the GAUSSIAN precludes the obtaining of the ghost energies, but the total BSSE related to the contribution of all hydrogen bonds is available. As such, this is very important in the CE analysis, mainly in the application of the equations proposed by Wells and Wilson [67] and Valiron and Meyer [68], for instance. The PCA study was developed through the version 6.0 of the UNSCRAMBLER software specific for multivariate analysis [113]. The QTAIM calculations were carried out by using the QTAIM routines implemented in the GAUSSIAN 03W [114], AIM 2000 1.0 [115], and AIMAll 11.05.16 [116] quantum software packages.

Results and discussion

Structural cooperativity

Figures 1 and 2 illustrate the optimized geometries of the C_2H_2···HCN···HF (**I**), C_2H_2···HCN···HCN (**II**), C_2H_4···HCN···HF (**IV**) and C_2H_4···HCN···HCN (**V**) trimeric complexes as well as the C_2H_2···HCN (**III**) and C_2H_4···HCN (**VI**) heterodimers. Moreover, the optimized geometries of the HCN···HCN (**VII**) and HCN···HF (**VIII**) heterodimers as well as of the HCN (**IX**), HF (**X**), C_2H_2 (**XI**) and C_2H_4 (**XII**) monomers are exhibited in Fig. 3. The values of the bond lengths obtained from the B3LYP/6-311++G(d,p) and BHandHLYP/6-311++G(d,p) (values in parentheses) calculations are also drawn. Firstly, the hydrogen bond distances should be analyzed carefully because their values give support to the prediction of the intermolecular strength. Independent if B3LYP/6-311++G(d,p) or BHandHLYP/6-311++G(d,p) is considered, the theoretical results show that the formation of the **I**–**V** complexes caused a reduction on the distance of the H···π H-bonds. However, this same trend is less critical in the N···HCN H-bonds because the application of the B3LYP/6-311++G(d,p) and BHandHLYP/6-311++G(d,p) calculations provided the values of 2.2086 Å and 2.1908 Å in **I** as well as 2.2051 Å and 2.1890 Å in **IV**, and these are considered slight changes in comparison with the results of 2.2298 Å and 2.2087 Å of the HCN···HCN homodimer. In direct consonance with **II** and **V**, the N···HF distances are also altered in comparison with the values in HCN···HF. In order to synthesize this discussion, in Fig. 4 how the distances of the hydrogen bonds π···H, N···HCN, and N···HF vary after formation of the trimolecular complexes are illustrated. It can be seen that the greatest variations on the H···π H-bonds occur in $\Delta R_{(\pi\cdots H,\mathbf{II}} - {}_{\pi\cdots H,\mathbf{III})}$ of **II** and $\Delta R_{(\pi\cdots H,\mathbf{V}} - {}_{\pi\cdots H,\mathbf{VI})}$ of **V** followed by $\Delta R_{(\pi\cdots H,\mathbf{I}} - {}_{\pi\cdots H,\mathbf{III})}$ of **I** and $\Delta R_{(\pi\cdots H,\mathbf{IV}} - {}_{\pi\cdots H,\mathbf{VI})}$ of **IV**. In addition, the N···HCN and N···HF distances are practically unaltered, wherein the π···H H-bonds are strengthened more than those formed by lone pairs of electrons as proton acceptors [117], and of course this is a very rare event. This counterbalanced behavior shows that the structural cooperativity is not manifested. In advance, the variations on the bond lengths of the proton-donors (HCN and HF) can be a suitable justification and this is what we are also hoping to demonstrate.

Likewise, it must be emphasized the function of the π bonds of the acetylene and ethylene or the nonbonding electron pair of the nitrogen as proton acceptors [118, 119] in order to know in which manner these molecular sites contribute to the hydrogen bond strength, and in addition, it is also vital to discover whether the structural basis of cooperativity is affected by this regard. In acetylene clusters, it can be seen in both B3LYP/6-311++G(d,p) and BHandHLYP/6-311++G(d,p) that all C≡C bond lengths are slightly increased, mainly in the trimers **I** and **II**. On the structural viewpoint, it is so natural that longer chains permit more accentuated molecular changes, but in regards to the proton receptors, only the π bonds of the acetylene and ethylene are affected because the lengths of the C≡N bonds of the hydrogen cyanide acid keep themselves practically unaltered. As aforesaid that the distances of the π···H H-bonds are so reduced after formation of the trimers, it is reasonable to admit that a substantial amount of π charge are transferred to the hydrogen cyanide, and thereby a partial loss of the π character in the acetylene (triple bond) and ethylene (double bond) must be considered. Some time ago, Ramos et al. [58, 120] have shown some theoretical results of π hydrogen-bonded complexes, where among them, the C_2H_2···HCN and C_2H_4···HCN heterodimers were studied at the MP2/6-311++G(d,p) level of theory. Instead of the distance of the π···H H-bonds, the distances between the carbon atom of the H–C bond oriented exactly to the midpoint of the

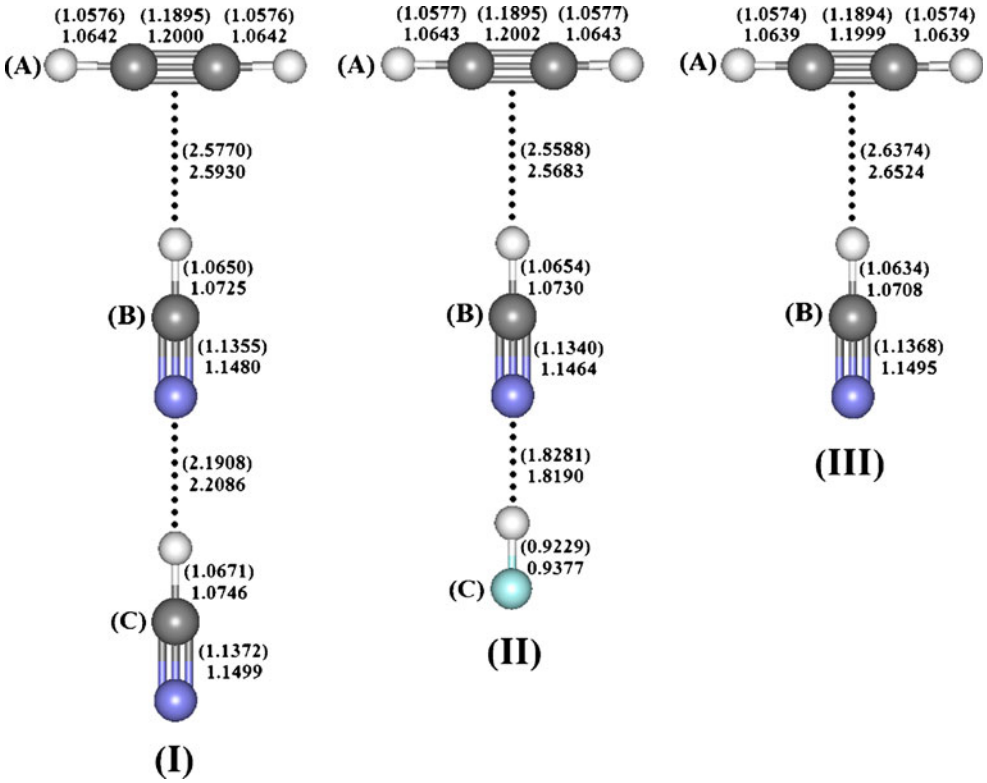

Fig. 1 Optimized geometries of the C_2H_2···HCN···HW clusters with W=CN (**I**) or F (**II**), as well as of the C_2H_2···HCN (**III**) heterodimer. These values were obtained from the B3LYP/6-311++G(d,p) and BHandHLYP/6-311++G(d,p) (in parentheses) levels of theory

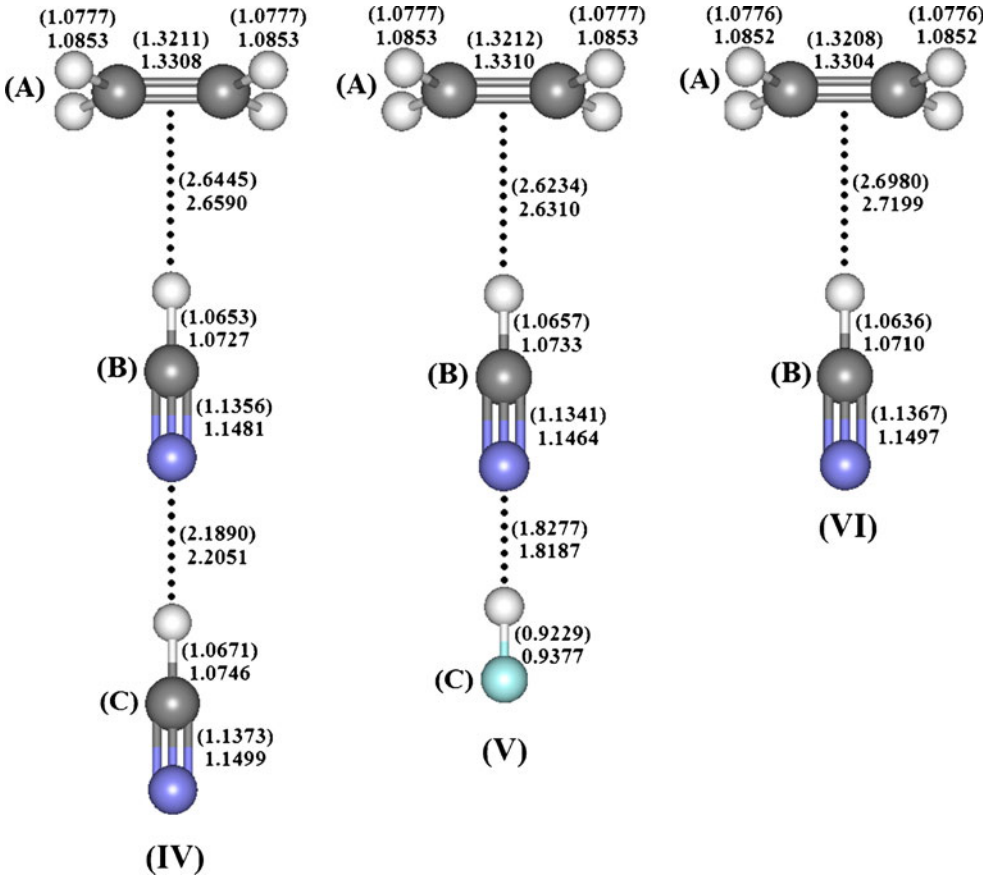

Fig. 2 Optimized geometries of the C_2H_4···HCN···HW clusters with W=CN (**IV**) or F (**V**), as well as of the C_2H_4···HCN (**VI**) heterodimer. These values were obtained from the B3LYP/6-311++G(d,p) and BHandHLYP/6-311++G(d,p) (in parentheses) levels of theory

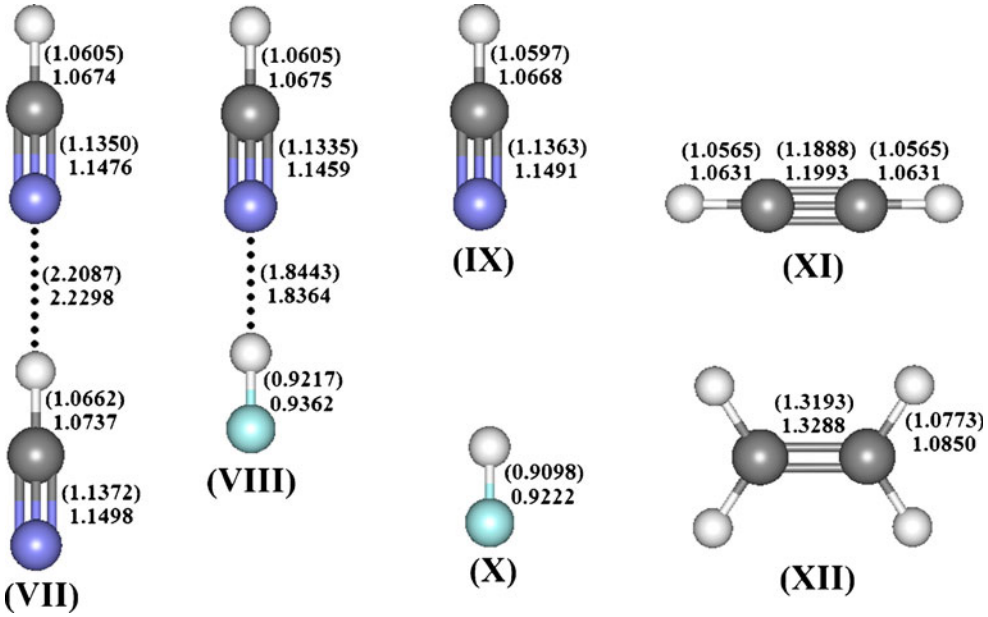

Fig. 3 Optimized geometries of the HCN···HW heterodimers with W=CN (**VII**) or F (**VIII**), as well as of the HCN (**IX**), HF (**X**), C_2H_2 (**XI**), and C_2H_4 (**XII**) monomers. These values were obtained from the B3LYP/6-311++G(d,p) and BHandHLYP/6-311++G(d,p) (in parentheses) levels of theory

C≡C bonds of the acetylene and ethylene were examined. For the C_2H_2···HCN complex, a good relationship between the experimental reference of 3.6560 Å [121] and the theoretical value of 3.6680 Å computed at the MP2/6-311++G(d,p) level of theory was demonstrated, but in general our results of 3.6421 Å and 3.6652 Å for **I** as well as 2.6413 Å and 2.6248 Å for **II** indicate that the distance C≡C···H–C is more efficiently reproduced by B3LYP/6-311++G(d,p) rather than BHandHLYP/6-311++G(d,p). However, we are not worried whether the distance C≡C···H–C influences or not on the cooperative effect. Actually, we do not believe that C≡C···H–C or C=C···H–C seems strong enough to do this in high level, but in an overview, it is important to emphasize that our values of

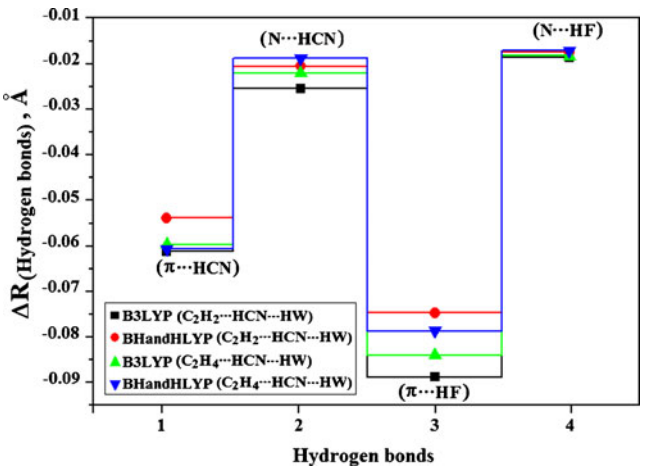

Fig. 4 Variation in H-bond distances within the C_2H_2···HCN···HW and C_2H_4···HCN···HW clusters with W=CN (**I** and **IV**) or F (**II** and **V**). These values were obtained from the B3LYP/6-311++G(d,p) and BHandHLYP/6-311++G(d,p) (in parentheses) levels of theory

3.7000 Å and 3.7610 Å ($r_{C–H}+R_{\pi\cdots H}$) for **III** and **VI** computed by BHandHLYP/6-311++G(d,p) can be considered accurate results. By this insight, indirectly the shortening of the C≡C···H–C must corroborate with the reduction of the π···H H-bonds, but this is justly irrefutable even if the bond length of $r_{C–H}$ is increased.

Hence, the most pronounced deformation in hydrogen complexes is the bond length enhancement ($\Delta r_{H–W}$) in the proton-donors (HW with W=CN and F) [50–53, 57, 58, 61–63, 117, 119]. Still according to Ramos et al. [120], the MP2/6-311++G(d,p) level of theory yielded $\Delta r_{H–W}$ results of 0.0030 Å for C_2H_2···HCN and C_2H_4···HCN, respectively. In this current work, however, the $\Delta r_{H–W}$ results vary from 0.0040 Å in **III** to 0.0042 Å in **V**, which were obtained through the B3LYP/6-311++G(d,p). This same analysis yielded results of 0.0037 Å (**III**) and 0.0039 Å (**V**) at the BHandHLYP/6-311++G(d,p) level of theory. Slight deformations were obtained at BHandHLYP by which shorter values for the $R_{H\cdots\pi}$ distances were calculated, i.e., nor is it always necessary that longer distances be related to weaker intermolecular interactions, but what would also lead to lowermost alterations on the structure in a whole. Regarding the trimers, Fig. 5 illustrates the bond length variations (Δr) on the π bonds (C≡C and C=C), HCN (B and C) and HF (C) proton-donors computed by both B3LYP/6-311++G(d,p) and BHandHLYP/6-311++G(d,p) levels. As can be seen, two sheer profiles indicate accentuated changes of 0.0131 Å and 0.0155 Å in $\Delta r_{(H–F,\mathbf{II}\ –\ H–F,\mathbf{X})}$ and $\Delta r_{(H–F,\mathbf{V}\ –\ H–F,\mathbf{X})}$, respectively. At first sight, it is quite impressive that the greatest variations on the π hydrogen bonds provoke perturbations not on the HCN, but indirectly on the HF molecule. In good agreement with the results reported by Li et al. [122], it can be seen that HCN behaves

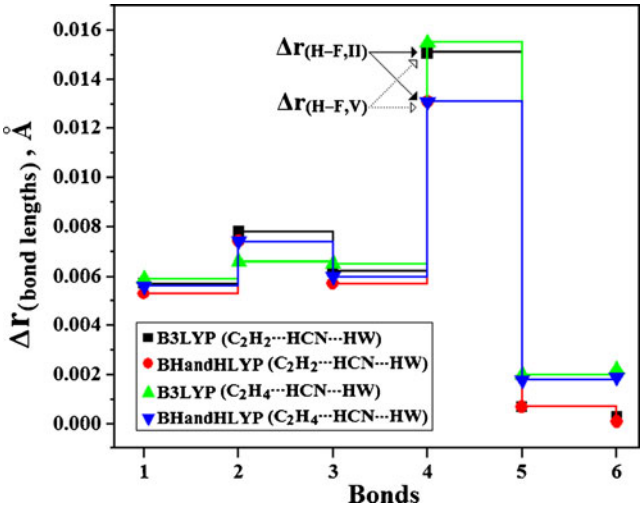

Fig. 5 Variation in lengths of the covalent bonds (C≡C, C=C, H−C, and H−F) within the C_2H_2···HCN···HW and C_2H_4···HCN···HW clusters with W=CN (**I** and **IV**) or F (**II** and **V**). These values were obtained from the B3LYP/6-311++G(d,p) and BHandHLYP/6-311++G(d,p) (in parentheses) levels of theory

as an inert mediator for cooperativity and HF represents the indispensable polar entity to the stronger hydrogen bond.

Vibrational cooperativity

By taking into account that the spectroscopy analysis is the irrefutable evidence of the structural behavior [123–125] as well as the vibrational essence of the hydrogen bond is manifested by the variations of the stretch frequencies of the proton-donors which can be shifted toward blue or red regions of the electronic spectrum, it is by conciliation between structure and vibration that we hope to interpret the cooperative effect, as can be seen in the works of Gong et al. [126] and Zabardasti et al. [127]. The computed values by B3LYP/6-311++G(d,p) and BHandHLYP/6-311++G(d,p) for the stretch frequencies and absorption intensities accompanied by their variations and ratios in the bimolecular complexes **III**, **VI**, **VII**, and **VIII** are organized in Tables 1 and 2, whereas in Tables 3 and 4 the results on the trimolecular complexes **I**, **II**, **IV**, and **V** are listed. It is well established that variations in the stretch frequencies upon the formation of intermolecular systems are evidenced with the appearing of the red-shifts and blue-shifts closely correlated with the increasing and decreasing of the bond lengths of the proton-donors [128]. In all of them, here either HCN or HF, their $\Delta\upsilon_{H-C}$ and $\Delta\upsilon_{H-F}$ oscillators are shifted to downward values after formation of the bimolecular and trimolecular hydrogen-bonded complexes, in which the red-shifts arise. As is clearly assumed, the enlargement of the bond lengths corroborates with such effect, and in fact, the most pronounced variations of 0.0131 Å and 0.0155 Å computed by B3LYP/6-311++G(d,p) and BHandHLYP/6-311++G(d,p) for $\Delta r_{H-W,C}$ of **II** are justified by the greatest red-shifts of –338.6 and –303.8 cm^{-1} [129]. Note that slight variations are also obtained by the BHandHLYP functional. Furthermore, less evident red-shifts are observed on $\Delta\upsilon_{H-C,B}$ and this occurs because the structure of the hydrogen cyanide remains almost unchanged.

By considering the modern characteristics of the hydrogen bonds, evidently the unsaturated bond of the acetylene and ethylene is a suitable electron source to interact intermolecularly [51, 58, 61, 120, 130, 131]. As such, a great variation on the oscillator $\Delta\upsilon_{\pi}$ would be expected, which is not verified because the red-shift values obtained by B3LYP/6-311++G(d,p) are in the range of –3.4 up to –4.8 cm^{-1}. Once again, revisiting the relationship between structural and vibrational parameters, we would like to discuss an unusual observation about the new vibrational modes, or commonly known as hydrogen bond stretch frequencies. As pointed out by Fig. 4, the variations in the hydrogen bond distances since the formation of the heterodimer up to heterotrimer reveal a drastic shortening on the $\Delta R_{(\pi\cdots H,\mathbf{II}\ -\ \pi\cdots H,\mathbf{III})}$ of **II** and $\Delta R_{(\pi\cdots H,\mathbf{V}\ -\ \pi\cdots H,\mathbf{VI})}$ of **V**. Precisely, these changes are peculiar to trimolecular complexes containing the terminal hydrofluoric acid. Indeed, this could lead to a vibrational

Table 1 Values of the stretch frequencies and absorption intensities of the C_2H_2···HCN (**III**), C_2H_4···HCN (**VI**) and HCN···HF (**VIII**) heterodimers and HCN···HCN (**VII**) homodimer obtained from the B3LYP/6-311++G(d,p) calculations

Modes	Hydrogen-bonded complexes			
	III	VI	VII	VIII
$\Delta\upsilon_{\pi}$	−3.4 (2058.8)	−3.5 (1680.4)	–	–
$I_{\pi t}/I_{\pi m}$	1.03 (1.03)	1.58 (1.58)	–	–
$\Delta\upsilon_{H-C,A}$	−59.2 (3393.7)	−62.6 (3390.3)	−92.9 (3360)	−308 (3787.7)
$I_{H-Ct,A}/I_{H-Cm,A}$	3.3 (221.7)	3.4 (231.2)	5.2 (353.7)	7.6 (1018.3)
$\upsilon_{\pi\cdots H}$	75.7	71.2	–	–
$I_{\pi\cdots H}$	0.42	0.35	–	–
$\upsilon_{N\cdots H-W}$	–	–	114.2	185.8
$I_{N\cdots H-W}$	–	–	2.0	4.8

Values of υ in cm^{-1} and I in $km.mol^{-1}$

Table 2 Values of the stretch frequencies and absorption intensities for the C_2H_2 HCN (**III**), C_2H_4 HCN (**VI**) and HCN HF (**VIII**) heterodimers and HCN HCN (**VII**) homodimer obtained from the BHandHLYP/6-311++G(d,p) calculations

Modes	Hydrogen-bonded complexes			
	III	VI	VII	VIII
$\Delta\upsilon_{\pi}$	−3.5 (2135.8)	−3.3 (1747.7)	–	–
$I_{\pi t}/I_{\pi m}$	1.09 (1.09)	0.93 (0.93)	–	–
$\Delta\upsilon_{H-C,A}$	−53.6 (3495.3)	−57.5 (3491.4)	−87.7 (3461.2)	−276.5 (4006.9)
$I_{H-Ct,A}/I_{H-Cm,A}$	2.86 (214.6)	2.99 (224.9)	4.7 (351.3)	6.3 (1016.8)
$\upsilon_{\pi\cdots H}$	81.1	76.6	–	–
$I_{\pi\cdots H}$	0.41	0.29	–	–
$\upsilon_{N\cdots H-W}$	–	–	122.0	188.0
$I_{N\cdots H-W}$	–	–	1.93	4.37

Values of υ in cm^{-1} and I in $km.mol^{-1}$

observation recognized as blue-shift by which the variation on the new stretching modes ($\Delta\upsilon_{\pi\cdots H}$) seems similar to those detected in proton-donors [132]. In these π···H attractions, such observation is not entirely reliable, although the shortening of the N···HCN and N···HF H-bonds are closely related to the blue-shifts of +15.6 and +12.5 cm^{-1} for **I** and **II**, as already widely documented in several works [133, 134]. This same tendency can also be demonstrated for those trimolecular complexes formed by ethylene independently whether the theoretical level used in this regard is the B3LYP/6-311++G(d,p) or BHandHLYP/6-311++G(d,p). So, the correlation between the variations on the bond lengths and vibrational displacements is not satisfactory, and due to this, the description of the vibrational cooperativity cannot be justly entrusted on the analysis of the intermolecular frequency shifts [135].

Electronic cooperativity

The energy analysis of the cooperative effect on **I**, **II**, **IV** and **V** was interpreted mathematically through the application of Eqs. 4 (SSFC) [67], 6, 7, 8 (Hankins, Moskowitz, and Stillinger) [70], and 10. In Table 5 all energy values at B3LYP/6-311++G(d,p) and BHandHLYP/6-311++G(d,p) with all of them corrected by the counterpoise calculations are listed, namely as $\Delta E^{CP}_{(A\cdots B\cdots C)}$, $\Delta^2E^{CP}_{(A\cdots B)}$, $\Delta^2E^{CP}_{(B\cdots C)}$, $\Delta^2E^{CP}_{(A\cdots C)}$, and $\Delta^3E^{CP}_{(A\cdots B\cdots C)}$. The nature of the cooperative effect is routinely explained in terms of energy distribution, and in according with the values gathered in Table 5, higher results of $\Delta^2E^{CP}_{(B\cdots C)}$ related to the N···HW H-bonds can be seen. To some extent, the cooperativity is feasible in **I** and **IV**, but in **II** and **V** absolutely not because the polar activity of the terminal hydrofluoric acid (B) distort the energy along the T-shaped structures. If we compute the difference between

Table 3 Values of the stretch frequencies and absorption intensities of the C_2H_2···HCN···HW (**I** and **II**) and C_2H_4···HCN···HW (**IV** and **V**) clusters obtained from B3LYP/6-311++G(d,p) calculations

Modes	Clusters			
	I	II	IV	V
$\Delta\upsilon_{\pi}$	−4 (2058)	−4.5 (2057.7)	−4.6 (1679.3)	−4.8 (1679.1)
$I_{\pi t}/I_{\pi m}$	1.84 (1.84)	1.97 (1.97)	1.49 (1.49)	1.58 (1.58)
$\Delta\upsilon_{H-C,B}$	−77.2 (3375.7)	−83.6 (3369.3)	−81.7 (3371.2)	−89.1 (3363.8)
$I_{H-Ct,B}/I_{H-Cm,B}$	2.5 (172.4)	4.9 (335.9)	2.41 (162)	5.3 (355.5)
$\Delta\upsilon_{H-W,C}$	−105.9 (3347)	−338.6 (3757.2)	−106.4 (3346.5)	−329 (3766.8)
$I_{H-Wt,C}/I_{H-Wm,C}$	7.5 (505.9)	8.7 (1138.4)	8.0 (538.1)	8.8 (1150.4)
$\upsilon_{\pi\cdots H}$	65.8	74.4	62.1	70.0
$\Delta\upsilon_{\pi\cdots H,I\text{-}III}$	−9.9	−8.6	−9.1	−1.2
$I_{\pi\cdots H}$	1.0	0.90	0.84	0.78
$I_{\pi\cdots H,I}/I_{\pi\cdots H,III}$	2.38	2.14	2.4	2.2
$\upsilon_{N\cdots H-W}$	129.8	198.3	129.2	198
$\Delta\upsilon_{N\cdots H-W}$	+15.6	+12.5	+15.2	+12.2
$I_{N\cdots H-W}$	0.92	3.80	1.10	4.04
$I_{N\cdots H-Wt}/I_{N\cdots H-Wd}$	0.45	0.8	0.54	1.99

Values of υ in cm^{-1} and I in $km.mol^{-1}$

Table 4 Values of the stretch frequencies and absorption intensities of the C_2H_2···HCN···HW (**I** and **II**) and C_2H_4···HCN···HW (**IV** and **V**) clusters obtained from BHandHLYP/6-311++G(d,p) calculations

Modes	Clusters			
	I	II	IV	V
$\Delta\upsilon_{\pi}$	−4,1 (2135.2)	−4.6 (2134.8)	−4.1(1746.9)	−4.5 (1746.5)
$I_{\pi t}/I_{\pi m}$	1.96 (1.96)	2.01 (2.01)	1.58 (1.58)	1.63 (1.63)
$\Delta\upsilon_{H-C,B}$	−70.1(3478.8)	−75 (3473.9)	−75.5 (3473.4)	−80.5 (3468.4)
$I_{H-Ct,B}/I_{H-Cm,B}$	2.2 (163.9)	3.98 (298.7)	2.0 (151.2)	4.2 (315.3)
$\Delta\upsilon_{H-X,C}$	−99.8(3449.1)	−303.8(3979.6)	−100.4 (3448.5)	−304.6 (3978.8)
$I_{H-Xt,C}/I_{H-Xm,C}$	6.4 (486.2)	7.0 (1130.7)	6.9 (517.7)	7.1 (1143.3)
$\upsilon_{\pi\cdots H}$	70.1	78.1	66.0	73.5
$\Delta\upsilon_{\pi\cdots H,I-III}$	−11.0	−8.0	−10.6	−3.1
$I_{\pi\cdots H}$	0.88	0.80	0.74	0.67
$I_{\pi\cdots H,I}/I_{\pi\cdots H,III}$	2.14	1.95	2.50	2.30
$\upsilon_{N\cdots H-W}$	137.7	200.7	136.6	200.3
$\Delta\upsilon_{N\cdots H-W}$	+15.7	+12.7	+14.6	+12.3
$I_{N\cdots H-W}$	0.93	3.40	1.0	3.65
$I_{N\cdots H-Wt}/I_{N\cdots H-Wd}$	0.48	0.70	0.56	1.89

Values of υ in cm^{-1} and I in $km.mol^{-1}$

$\Delta E^{CP}_{(A\cdots B\cdots C)}$ and $\Delta^3E^{CP}_{(A\cdots B\cdots C)}$ by means of Eq. 10, the sum of the $\Delta^2E^{CP}_{(A\cdots B)}$, $\Delta 2E^{CP}_{(B\cdots C)}$, and $\Delta^2E^{CP}_{(A\cdots C)}$ can be quantified. In other words, the energy distributed along the N···HCN and N···HF H-bonds can be estimated. Indeed, the values of –0.009639 or –25.30 (**I**), –0.014947 or –29.23 (**II**), –0.009269 or –24.33 (**IV**), and –0.015654 Hartree or –41.10 $kJ.mol^{-1}$ (**V**) determined by B3LYP/6-311++G(d,p) as well as those obtained from the BHandHLYP/6-311++G(d,p) level can be classified as high energies, which in some cases are equivalent to noncovalent interactions [136, 137] such as those formed by rare gases [138]. By taking into account this insight, a skilful criterion should be elaborated to discriminate which of $\Delta^2E^{CP}_{(A\cdots B)}$, $\Delta^2E^{CP}_{(B\cdots C)}$, and $\Delta^2E^{CP}_{(A\cdots C)}$ are answerable by the energy accumulation along the C_nH_m···HCN···HW complexes.

Figure 6 illustrates the PCA profile in which the relationships between the **I**, **II**, **IV**, **V** (intermolecular systems as variables) and $\Delta^2E^{CP}_{(A\cdots B)}$, $\Delta^2E^{CP}_{(B\cdots C)}$, $\Delta^2E^{CP}_{(A\cdots C)}$, and

Table 5 Values of the interaction energies and ghost energies of the C_2H_2···HCN···HW (**I** and **II**) and C_2H_4···HCN···HW (**IV** and **V**) clusters at both B3LYP/6-311++G(d,p) and BHandHLYP/6-311++G(d,p) levels of theory

Parameters	Trimolecular hydrogen-bonded complexes			
	I	II	IV	V
$\Delta E^{CP}_{(A\cdots B\cdots C)}$ [a]	−264.2764452	−271.3093016	−265.5347178	−272.5680698
	(–264.1028126)	(–271.1538172)	(–265.3572092)	(–272.4080837)
$\Delta^2E^{CP}_{(A\cdots B)}$ [b]	−0.0026801	−0.0026626	−0.0024665	−0.0024482
	(–0.0030910)	(–0.0030849)	(–0.0029964)	(–0.0029817)
$\Delta^2E^{CP}_{(B\cdots C)}$ [b]	−0.0067624	−0.0120400	−0.0067601	−0.0120396
	(–0.0075700)	(–0.0125329)	(–0.0075690)	(–0.0124227)
$\Delta^2E^{CP}_{(A\cdots C)}$ [b]	−0.0001973	−0.0002471	−0.0000428	−0.0001842
	(–0.0001988)	(–0.0003678)	(–0.0001560)	(–0.0002500)
$\Delta^3E^{CP}_{(A\cdots B\cdots C)}$ [c]	−264.2668058	−271.2943545	−265.5254484	−272.5533980
	(–264.0919538)	(–271.1440014)	(–265.3464878)	(–272.3924293)

All values are given in Hartree; $\Delta E^{CP}_{TOTAL} = \Delta E^{CP}_{(A\cdots B\cdots C)^a} - \Delta^3E^{CP}_{(A\cdots B\cdots C)^c}$;

[a] SSFC

[b] Hankins, Moskowitz, and Stillinger (ref [70])

[c] Eq. 10

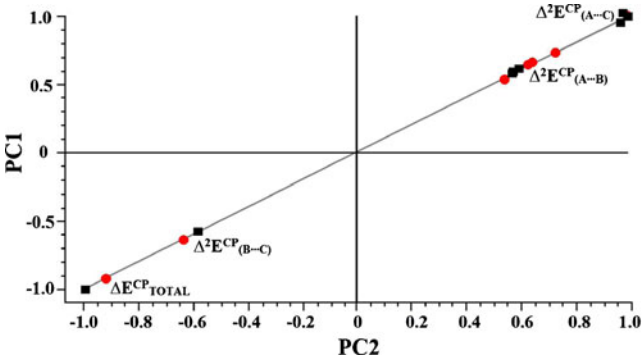

Fig. 6 Plotted graph of the PCA analysis of the H-bond energies in both (B3LYP/6-311++G(d,p) (black squares) and BHandHLYP/6-311++G(d,p) (red circles) calculations

ΔE^{CP}_{TOTAL} (cooperative terms as samples) in both B3LYP/6-311++G(d,p) or BHandHLYP/6-311++G(d,p) levels are divulged. Some time ago, da Silva et al. [139] documented the versatility and efficiency of chemometric methods to examine theoretical results of rotational constants in comparison with some available experimental data. Meanwhile, Araújo et al. [140] have also performed a chemometry study of low H-bond energies in a group of intermolecular systems quite similar to the **III**, **VII**, and **VIII** heterodimers. Analogously, we also published a similar investigation related to specific molecular parameters of heterocyclic hydrogen-bonded complexes [141]. In this current work, however, among the $\Delta^2E^{CP}_{(A\cdots B)}$, $\Delta^2E^{CP}_{(B\cdots C)}$ and $\Delta^2E^{CP}_{(A\cdots C)}$ terms examined here, we are searching for the most important contributor that disables the cooperative effect. However, it should be emphasized that albeit the missing of experimental references is a consummate fact, this is not an impediment to execute our investigation [141]. So, the $\Delta^2E^{CP}_{(B\cdots C)}$ located at left axis indicates a negative contribution, which in practice leads to a diminishing of the cooperative effect. In other words, the distortion caused by the high polarizability of the hydrofluoric acid inhibits the equivalent distribution of energy. Moreover, the similarity between $\Delta^2E^{CP}_{(B\cdots C)}$ and ΔE^{CP}_{TOTAL} lead us to affirm that the larger contribution against the cooperative effect comes from hydrofluoric acid. On the other hand, $\Delta^2E^{CP}_{(A\cdots B)}$ and $\Delta^2E^{CP}_{(A\cdots C)}$ are positive cooperative agents. In the loading results symbolized by Eqs. 13 and 14, it can be seen that **II** and **V** are dominant variables containing 99 and 95 % of the total variance for PC1 when the respective B3LYP/6-311++G(d,p) and BHandHLYP/6-311++G(d,p) calculations are used.

$$PC1_{(B3LYP)} = 0.36(\mathbf{I}) + 0.61(\mathbf{II}) + 0.35(\mathbf{IV}) + 0.60(\mathbf{V}) \quad (13)$$

$$PC1_{(BHandHLYP)} = 0.41(\mathbf{I}) + 0.47(\mathbf{II}) + 0.41(\mathbf{IV}) + 0.65(\mathbf{V}) \quad (14)$$

Actually, we are aware that our universe of study is much reduced, but in a qualitative overview our investigation corroborates closely with the structural and vibrational analysis [129] in order to affirm that hydrofluoric acid promotes the addictive effect, whose main characteristic is the resistance against the cooperativity. So, we would like to consider that some discarded effects can be relevant, such as outliers or samples with multiple factors embodied into them. However, once again we wish to affirm that our intention was not taken upon with the purpose of a detailed chemometric analysis, but just a cursory one likewise efficient to determine the most important factor inherent to the cooperative effect of the $C_nH_m\cdots HCN\cdots HW$ clusters.

Topological cooperativity

Throughout this paper, great attention has been dedicated to the donors and acceptors of protons concerning the following bonds: π (acetylene and ethylene), H–C (hydrogen cyanide), and H–W (hydrofluoric acid or hydrogen cyanide) [142–145]. In Table 6 the QTAIM topological results for these bonds upon the formation of the **I**, **II**, **IV**, and **V** clusters are organized. Many years ago, Cremer and Kraka [146, 147] elaborated a clear vision about the concentration of charge between atoms in concordance with the electronic energy $H_{(r)}$, in which the kinetic $G_{(r)}$ and potential $U_{(r)}$ moieties are held as [148]:

$$H_{(r)} = G_{(r)} + U_{(r)} \quad (15)$$

So, bonds containing high charge concentration outweigh the potential contributions, which in this case the electronic energy profile is always negative. Otherwise, intermolecular contacts are currently identified by means of the dominant kinetic energy, which in this context yields a positive electronic energy. As can be seen in Table 6, all C=C, C≡C, H–W, and H–C bonds are characterized as covalent because their $H_{(r)}$ values are negative. This is, indeed, a quantum mechanics justification for the covalent character of these bonds, wherein high charge densities corroborates well with this finding. Moreover, in order to corroborate with this topological analysis, it is clearly seen that negative Laplacian values are also a hint of the valence shell charge concentration [149].

Analyzing the results of the Tables 7 and 8, if we compare the π bonds of the acetylene and ethylene, a constancy on its electronic density is easily noted, which denotes slight topological perturbations in these bond paths [150]. In corroboration with this, the constancy of the ellipticity (ε) also reinforces the cooperativity on the π bonds, although the curvature ($\varepsilon = \lambda_1/\lambda_2 - 1$) computed on C≡C is lower in comparison with C=C, which is an exception widely known [151]. About the action of the H–W proton-donor, the electronic density on the terminal hydrogen cyanide is slightly modified, whereas an opposite behavior is observed on the hydrofluoric acid. Note that a substantial reduction on

Table 6 Values of the QTAIM topological parameters of the C_2H_2···HCN···HW (**I** and **II**) and C_2H_4···HCN···HW (**IV** and **V**) clusters at both B3LYP/6-311++G(d,p) and BHandHLYP/6-311++G(d,p) levels of theory

	Bonds	QTAIM parameters					
		$\rho_{(r)}$	$\nabla^2\rho_{(r)}$	ε	$G_{(r)}$	$U_{(r)}$	$H_{(r)}$
I	C≡C	0.41168	−1.24325	0.00656	0.28326	−0.87735	−0.59409
		(0.42111)	(–1.30970)	(0.00623)	(0.29613)	(–0.91969)	(–0.62356)
	H–C	0.28413	−1.06043	0.00018	0.02524	−0.31559	−0.29035
		(0.29147)	(–1.13917)	(0.00019)	(0.02369)	(–0.33217)	(–0.30848)
	H–W	0.28267	−1.05303	0.00000	0.02498	−0.31323	−0.28825
		(0.28993)	(–1.13199)	(0.00000)	(0.02344)	(–0.32988)	(–0.30644)
II	C≡C	0.41160	−1.24279	0.00709	0.28311	−0.87693	−0.59382
		(0.42093)	(–1.30894)	(0.00667)	(0.29587)	(–0.91899)	(–0.62312)
	H–C	0.28405	−1.06349	0.00018	0.02468	−0.31523	−0.29055
		(0.29148)	(–1.14298)	(0.00018)	(0.02320)	(–0.33215)	(–0.30895)
	H–W	0.34586	−2.59154	0.00000	0.08213	−0.81214	−0.73001
		(0.35918)	(–2.89163)	(0.00000)	(0.08156)	(–0.88603)	(–0.80447)
IV	C=C	0.34257	−1.02226	0.32389	0.13670	−0.52897	−0.39227
		(0.35266)	(–1.11077)	(0.35199)	(0.14065)	(–0.55899)	(–0.41834)
	H–C	0.28395	−1.05878	0.00003	0.02525	−0.31519	−0.28994
		(0.29123)	(–1.13734)	(0.00004)	(0.02368)	(–0.33169)	(–0.30800)
	H–W	0.28267	−1.05308	0.00000	0.02498	−0.31324	−0.28826
		(0.28899)	(–1.13194)	(0.00000)	(0.02344)	(–0.32986)	(–0.30642)
V	C=C	0.34248	−1.02193	0.32354	0.13663	−0.52873	−0.39210
		(0.35242)	(–1.10965)	(0.35154)	(0.14044)	(–0.55829)	(–0.41785)
	H–C	0.28382	−1.06163	0.00004	0.02469	−0.31478	−0.29009
		(0.29124)	(–1.14124)	(0.00004)	(0.02320)	(–0.33171)	(–0.30851)
	H–W	0.34581	−2.59141	0.00000	0.08213	−0.81210	−0.72997
		(0.35905)	(–2.89164)	(0.00000)	(0.08153)	(–0.88597)	(–0.80444)

Values of $\rho_{(r)}$ in a_o^3 and $\nabla^2\rho_{(r)}$ in a_o^5; BHandHLYP/6-311++G(d,p) results in parentheses

the electronic density of the hydrofluoric acid was detected. This statement accords well with the drastic increase in its bond length followed by the large red-shifted frequencies previously discussed in this work. As we can see, all hydrogen bonds were modeled in accordance with their topologies, by which the low amounts of electronic density and positive Laplacian fields were quantified, whose values are organized in Table 9 and illustrated in Fig. 7 (**a**=contour line of electronic density; **b**=relief map of the electronic density). This is a traditional benchmark well divulged among all theoretical chemists as an essential tool to characterize the existence of intermolecular contacts, mainly those formed by hydrogen bond containing vestiges of covalence within its bond path [152].

Since the first investigations of Lewis [153], Pauling [154], Pimentel and McClallen [155], up to the most recent treaty [48], covalency in hydrogen bond is considered one of the most worthy intermolecular phenomena [156], as well as wishful to be found in any chemical system in the nature. As can be seen, all positive values of $H_{(r)}$ indicate noncovalent profiles in the **I-VII** systems, either bimolecular or trimolecular. However, by the application of B3LYP/6-311++G(d,p) or BHandHLYP/6-311++G(d,p), it can be noted that all electronic density values in range of 0.0312−0.0331 e/a_o^3 for N···H–W reflect the polarizability of the terminal hydrofluoric acid. In order to justify this charge density bulging, it could be that a minimum or partial covalent character emerges? Unfortunately, only a covalent trend is exhibited. In accordance with Grabrowski et al. [157], the ratio $-G_{(r)}/U_{(r)}$ is a electronic balance well adapted to evaluate the covalent character of intermolecular interactions as follows: *i*) $-G_{(r)}/U_{(r)}>1$ (noncovalent); *ii*) $0.5<-G_{(r)}/U_{(r)}<1$ (partially covalent); *iii*) $-G_{(r)}/U_{(r)}<0.5$ (totally covalent) [158]. In Fig. 8 the relationship between the ratios $-G_{(r)}/U_{(r)}$ and the values of the intermolecular distances (R) computed in both B3LYP/6-311++G(d,p) and BHandHLYP/6-311++G(d,p) levels of theory are plotted:

$$-G_{(r)}\Big/U_{(r)} = 1.201R^2-5.843R+6.655,\ \ R^2=0.987. \quad (16)$$

This is, undoubtedly, a nonlinear relationship with a quadratic profile, where the strongest hydrogen bonds are recognized as being N···H–F, in which the proximity of $-G_{(r)}/U_{(r)}$ to

Table 7 Values of the QTAIM topological parameters of the C_2H_2···HCN (**III**), C_2H_4···HCN (**VI**) and HCN···HF (**VIII**) heterodimers and HCN···HCN (**VII**) homodimer at both B3LYP/6-311++G(d,p) and BHandHLYP/6-311++G(d,p) levels of theory

Values of $\rho_{(r)}$ in a_o^3 and $\nabla^2\rho_{(r)}$ in a_o^5; BHandHLYP/6-311++G(d,p) results in parentheses

	Bonds	QTAIM parameters					
		$\rho_{(r)}$	$\nabla^2\rho_{(r)}$	ε	$G_{(r)}$	$U_{(r)}$	$H_{(r)}$
III	C≡C	0.41162	−1.24229	0.00538	0.28339	−0.87737	−0.59398
		(0.4210)	(–1.30865)	(0.00511)	(0.29627)	(–0.91969)	(–0.62342)
	H–C	0.28438	−1.05249	0.00020	0.02662	−0.31635	−0.28973
		(0.29165)	(–1.12867)	(0.00021)	(0.02516)	(–0.33250)	(–0.30734)
VI	C=C	0.34280	−1.02360	0.32519	0.13694	−0.52978	−0.39284
		(0.35283)	(–1.11165)	(0.35323)	(0.14083)	(–0.55958)	(–0.41875)
	H–C	0.28423	−1.05105	0.00002	0.02663	−0.31603	−0.28940
		(0.29148)	(–1.12712)	(0.00003)	(0.02518)	(–0.33216)	(–0.31058)
VII	H–W	0.28317	−1.05473	0.00000	0.02519	−0.31408	−0.28889
		(0.29042)	(–1.13342)	(0.00000)	(0.02367)	(–0.33069)	(–0.30702)
VIII	H–W	0.34789	−2.61281	0.00000	0.08213	−0.81747	−0.73534
		(0.36118)	(–2.91011)	(0.00000)	(0.08171)	(–0.89096)	(–0.80925)

1 is almost attained, i.e., the respective values of 0.9963 and 0.9966 for **II** and **V** were obtained at the B3LYP/6-311++G(d,p) level of theory. Because the covalence degree is assumed when the hydrogen bond distances vary between 1.20-1.80 Å [157] or 1.62-1.96 Å [159], even so we wish to highlight the tendency of the partial covalent character in N···H–F. This is a certification that the terminal hydrofluoric acid incites to a distortion on the polarizability of the **II** and **V** clusters, in which the cooperative effect is repressed. On the contrary, the N···H–CN medium strength hydrogen bonds and mainly the π···H–CN weak ones are [160], in fact, noncovalent interactions are answerable to preserve the mutual charge distribution and the cooperative effect on all clusters examined in this work. Furthermore, it is evident that the interaction strength can be accounted justly via contrast of the H-bond energy and each intermolecular electronic density, as pointed out by Grabowski and others in several investigations [161–163]. In our current work, the values of Δ^2E^{CP} determined on the basis of Eqs. (6) and (7) (Hankins, Moskowitz and Stillinger's approach) [70] are linearly correlated with the QTAIM electronic densities [164–170], as illustrated by Fig. 9 and fitted mathematically by Eqs. (17) and (18). The straggled location of N···HF is one more indication about the strength of this hydrogen bond, and in addition, this profile represents the weakening of the cooperative effect.

$$\Delta^2E^{CP} = -0.375\rho_{(r)} + 5.3 \times 10^{-5}, \quad R^2 = 0.982 \text{ at B3LYP}/6{-}311{+}{+}G(d,p) \tag{17}$$

$$\Delta^2E^{CP} = -0.406\rho_{(r)} - 1.5 \times 10^{-4}, \quad R^2 = 0.979 \text{ at BHandHLYP}/6{-}311{+}{+}G(d,p) \tag{18}$$

However, it should be noted that distorted correlations are also yielded, e.g., instead of a linear profile a parabolic relationship between H-bond energy and intermolecular electronic density can be demonstrated [171]. In this context but also by assuming the possibility to predict the hydrogen bond strength (ΔE) [172, 173] through the association (Δmol) between vibrational modes and QTAIM topography parameters [156, 160, 174] in accordance with Eq. (19),

Table 8 Values of the QTAIM topological parameters of the HCN (**IX**), HF (**X**), C_2H_2 (**XI**), and C_2H_4 (**XII**) monomers at both B3LYP/6-311++G(d,p) and BHandHLYP/6-311++G(d,p) levels of theory

Values of $\rho_{(r)}$ in a_o^3 and $\nabla^2\rho_{(r)}$ in a_o^5; BHandHLYP/6-311++G(d,p) results in parentheses

	Bonds	QTAIM parameters					
		$\rho_{(r)}$	$\nabla^2\rho_{(r)}$	ε	$G_{(r)}$	$U_{(r)}$	$H_{(r)}$
IX	H–C	0.28637	−1.05904	0.00000	0.02785	−0.32047	−0.29262
		(0.29350)	(–1.13262)	(0.00000)	(0.02649)	(–0.33614)	(–0.30965)
X	H–F	0.36950	−2.79984	0.00000	0.08367	−0.86729	−0.78362
		(0.38213)	(–3.05467)	(0.00000)	(0.08449)	(–0.93265)	(–0.84816)
XI	C≡C	0.41172	−1.24089	0.00000	0.28406	−0.87834	−0.59428
		(0.42117)	(–1.30736)	(0.00000)	(0.29693)	(–0.92069)	(–0.62376)
XII	C=C	0.34376	−1.02855	0.33039	0.13785	−0.53284	−0.39499
		(0.35377)	(–1.11668)	(0.35805)	(0.14168)	(–0.56254)	(–0.42086)

Table 9 Values of the QTAIM topological parameters of the C_2H_2···HCN···HW (**I** and **II**) and C_2H_4···HCN···HW (**IV** and **V**) clusters, C_2H_2 HCN (**III**), C_2H_4 HCN (**VI**) and HCN HF (**VIII**) heterodimers, and HCN HCN (**VII**) homodimer at both B3LYP/6-311++G(d,p) and BHandHLYP/6-311++G(d,p) levels of theory

	Bonds	QTAIM parameters					
		$\rho_{(r)}$	$\nabla^2\rho_{(r)}$	ε	$G_{(r)}$	$U_{(r)}$	$H_{(r)}$
I	π···H	0.00829	0.02245	0.31975	0.00427	−0.00294	0.00133
		(0.00841)	(0.02387)	(0.30118)	(0.00454)	(–0.00312)	(0.00142)
	N···H–W	0.01468	0.05301	0.00029	0.01038	−0.00750	0.00288
		(0.01486)	(0.05700)	(0.00034)	(0.01114)	(–0.00803)	(0.00311)
II	π···H	0.00867	0.02366	0.32503	0.00448	−0.00305	0.00143
		(0.00869)	(0.02481)	(0.30438)	(0.00470)	(–0.00320)	(0.00150)
	N···H–W	0.03309	0.10901	0.00011	0.02714	−0.02704	0.00010
		(0.03122)	(0.11372)	(0.00012)	(0.02741)	(–0.02640)	(0.00101)
III	π···H	0.007411	0.01970	0.30764	0.00380	−0.00268	0.00112
		(0.00756)	(0.02107)	(0.02107)	(0.00406)	(–0.00285)	(0.00121)
IV	π···H	0.00773	0.01788	0.47299	0.00352	−0.00257	0.00095
		(0.00787)	(0.01890)	(0.45642)	(0.00373)	(–0.00274)	(0.00009)
	N···H–W	0.01479	0.05348	0.00018	0.01048	−0.00759	0.00289
		(0.01493)	(0.05726)	(0.00025)	(0.01119)	(–0.00808)	(0.00311)
V	π···H	0.00811	0.01891	0.48162	0.00370	−0.00267	0.00103
		(0.00817)	(0.01974)	(0.46206)	(0.00387)	(–0.00281)	(0.00106)
	N···H–W	0.03312	0.10905	0.00000	0.02717	−0.02708	0.00009
		(0.03127)	(0.11376)	(0.00000)	(0.02744)	(–0.02644)	(0.00100)
VI	π···H	0.00689	0.01580	0.45494	0.00315	−0.00236	0.00079
		(0.00712)	(0.01695)	(0.44313)	(0.00338)	(–0.00253)	(0.00085)
VII	N···H–W	0.01395	0.05046	0.00000	0.00982	−0.00703	0.00279
		(0.01422)	(0.05465)	(0.00000)	(0.01062)	(–0.00758)	(0.00304)
VIII	N···H–W	0.03152	0.10659	0.00000	0.02594	−0.02522	0.00072
		(0.02983)	(0.11114)	(0.00001)	(0.02626)	(–0.02473)	(0.00153)

Values of $\rho_{(r)}$ in a_o^3 and $\nabla^2\rho_{(r)}$ in a_o^5; BHandHLYP/6-311++G(d,p) results in parentheses

usually a linear correlation is assumed in order to normalize the characteristics of the proton-donors.

$$\Delta\text{mol}=\left[\left(|\Delta\upsilon|/\upsilon_o\right)^2+\left(\left|\Delta\rho_{(r)}\right|/\rho_{(r)o}\right)^2+\left(\left|\Delta\nabla^2\rho_{(r)}\right|/\nabla^2\rho_{(r)o}\right)^2\right]^{1/2} \quad (19)$$

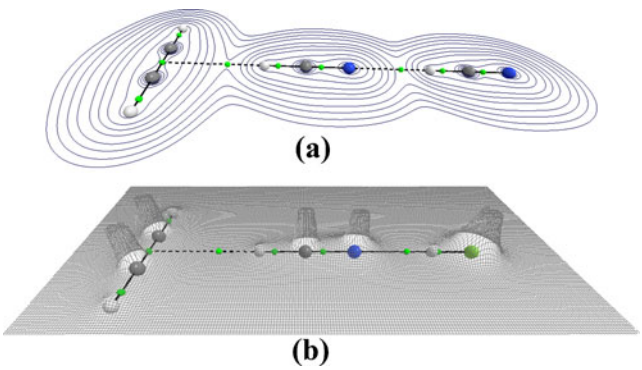

Fig. 7 Contour line (**a**) and relief map (**b**) of the electronic density for the C_2H_2···HCN···HCN and C_2H_2···HCN···HF clusters obtained from QTAIM topological integrations

Unlike linear projections, it may be noted in Fig. 10 that an exponential decay abridged by two profiles of first order

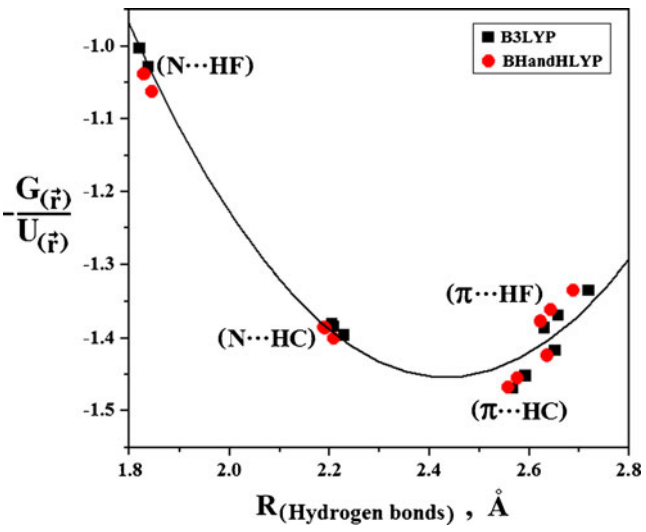

Fig. 8 Relationship between the ratios $-G_{(r)}/U_{(r)}$ and the values of the intermolecular distances (R) of the C_2H_2···HCN···HW and C_2H_4···HCN···HW clusters obtained from B3LYP/6-311++G(d,p) and BHandHLYP/6-311++G(d,p) levels of theory

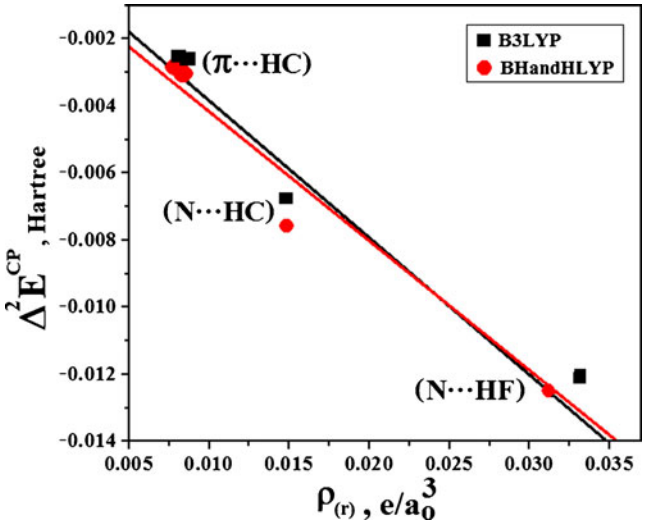

Fig. 9 Relationship between the values of the BSSE-corrected H-bond energies (Hankins, Moskowitz and Stillinger) and electronic densities computed in each intermolecular critical point at the B3LYP/6-311++G(d,p) and BHandHLYP/6-311++G(d,p) levels of theory for the C_2H_2···HCN···HW and C_2H_4···HCN···HW clusters, as well as for the HCN···HCN homodimer and HCN···HF heterodimer [160–170]

is noticed. Surely, this non-linear trend is another fact that justifies the distortion of the cooperative effect, due in part, to the extremist HF. Despite this exceptional case, the interaction strength can be designed by taking into account the intense vibrational displacements and drastic topological deformations on the terminal hydrofluoric acid.

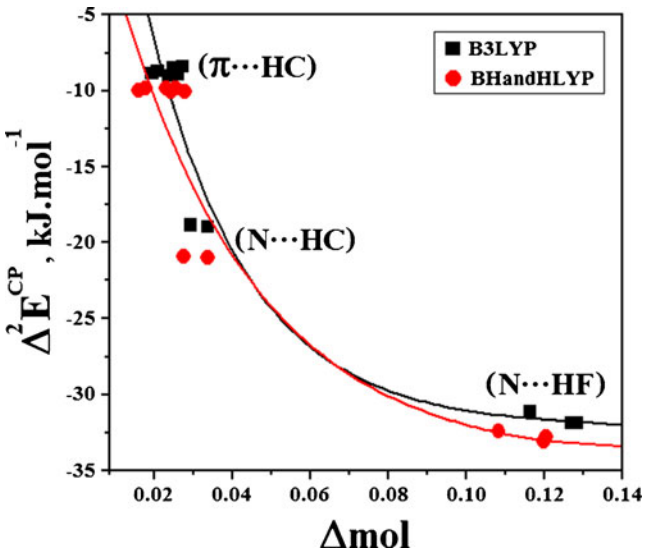

Fig. 10 Relationship between the values of the BSSE-corrected H-bond energies (Hankins, Moskowitz and Stillinger) and the results of the molecular parameter (Δmol=infrared spectrum+QTAIM) at the B3LYP/6-311++G(d,p) and BHandHLYP/6-311++G(d,p) levels of theory for the C_2H_2···HCN···HW and C_2H_4···HCN···HW clusters

Note that B3LYP/6-311++G(d,p) provides the best correlation between Δ^2E^{CP} and Δmol.

$$\Delta^2E^{CP} = -31.93 + 60.43e^{-\left(\Delta mol \middle/ 0.025\right)}, \quad R^2 = 0.93 \text{ at } B3LYP\middle/6{-}311++G(d,p) \tag{20}$$

$$\Delta^2E^{CP} = -34.36 + 50.64e^{-\left(\Delta mol \middle/ 0.030\right)}, \quad R^2 = 0.89 \text{ at } BHandHLYP\middle/6{-}311++G(d,p) \tag{21}$$

Conclusions

In this work, density functional calculations represented by means of the two hybrids B3LYP and BHandHLYP in association with the Pople's 6-311++G(d,p) composed our standard levels of theory to propose a novel theoretical interpretation about the cooperative effect on heteroclusters. In the structural analysis of the C_nH_m···HCN···HW clusters with n=2 (acetylene), m=2, or 4 (ethylene), and W=F (hydrofluoric acid) or CN (hydrogen cyanide), the most protuberant bond length change was found on HF. In line with this, the examination of the harmonic infrared spectrum indicates the existence of larger red-shifted frequencies at HF, which may be treated as the most active proton-donor in this regard. Additionally, the cooperative effect measurements in concordance with the algebraic formulations of VMFC and SSFC have shown satisfactory profiles, where besides, all of them were carefully re-examined through the PCA chemometric technique. By this context, it was concluded that N···HF H-bond contributed decisively to explain the maximum data variance. Thus, it was quoted that a strongest hydrogen bond like that could generate a covalent character on the C_2H_2···HCN···HF and C_2H_4···HCN···HF clusters. The strength of the N···HF hydrogen bond was interpreted in light of the QTAIM topological parameters, such as potential and kinetic energy components. As such, no covalent profile was found, although it may be highlighted that a slight trend about it has been discovered. In an overview, the molecular deformation on the C_nH_m···HCN···HW clusters is not devoted to covalence, but actually to a strong hydrogen bond formed by the high polarizalibity of the hydrofluoric acid. Although the relationship between the interaction energy versus vibrational and topology parameters is nonlinear, an exponential behavior was successfully modeled.

Acknowledgments The authors would like to thank CNPq (*Conselho Nacional de Desenvolvimento Científico e Tecnológico*) Brazilian Funding Agency. This works was funded in accordance with the document number 310331/2009-9 of the '*Produtividade em Desenvolvimento Tecnológico e Extensão Inovadora* – DT 2009' programme supported by the CNPq agency.

References

1. Contreras-García J, Johnson ER, Keinan S, Chaudret R, Piquemal J-P, Beratan DN, Yang W (2011) J Chem Theory Comput 7:625–632
2. Ilnicka A, Sadlej J (2012) Struct Chem 23:1323–1332
3. Scheiner S (2012) Acc Chem Res 46:280–288
4. Rajter RF, French RH (2008) J Phys Conf Ser 94:012001–01212
5. Gung BW, Xue X, Zou Y (2007) J Org Chem 72:2469–2475
6. Oliveira BG, Vasconcellos MLAA (2009) Inorg Chem Commun 12:1142–1144
7. Goymer P (2012) Nature Chem 4:863–864
8. Martin TW, Derewenda ZS (1999) Nature 6:403–406
9. Xiaofeng C, Dawei J, Li S (2009) Chin J Chem Edu 8:6–10
10. Oliveira BG, Araújo RCMU, Carvalho AB, Ramos MN, Hernandes MZ, Cavalcante KR (2005) J Mol Struct (THEOCHEM) 802:91–97
11. Filho EBA (2007) Ventura E, do Monte SA, Oliveira BG, Junior CGL, Rocha GB, Vasconcellos MLAA. Chem Phys Lett 449:336–340
12. Xue D, Ratajczak H (2005) J Mol Struct (THEOCHEM) 716:207–210
13. Kuhn B, Mohr P, Stahl M (2010) J Med Chem 53:2601–2611
14. Wilson AJ (2011) Nature Chem 3:193–194
15. Raymond KN (2009) Nature 460:585–586
16. Lehn J-M (1995) Supramolecular chemistry: concepts and perspectives. Wiley-VCH, Weinheim
17. Steed JW, Gale PA (2012) Supramolecular chemistry: from molecules to nanomaterials. Wiley-VCH, Weinheim
18. Ganguly P, Desiraju GR (2008) Chem Asian J 3:868–880
19. Shi J, Gao Y, Yang Z, Xu B (2011) Beilstein J Org Chem 7:167–172
20. Müller S, Kumari S, Rodriguez R, Balasubramanian S (2010) Nat Chem 2:1095–1098
21. Borho N, Suhm MA (2004) Phys Chem Phys Chem 6:2885–2890
22. Qureshi RN, Kok WT (2011) Anal Bioanal Chem 399:1401–1411
23. Goel S, Velizhanin KA, Piryatinski A, Tretiak S, Ivanov SA (2010) J Phys Chem Lett 1:927–931
24. Sophy KB, Kuo J-L (2009) J Chem Phys 131:224307–224315
25. Guedes RC, do Couto PC, Costa Cabral BJ (2003) J Chem Phys 118:1272–1282
26. Dykstra CE (1996) J Mol Struct (THEOCHEM) 362:1–6
27. Frontera A, Quiñonero D, Costa A, Ballester P, Deyà PM (2007) New J Chem 31:556–560
28. Tielrooij KJ, Garcia-Araez N, Bonn M, Bakker HJ (2010) Science 328:1006–1009
29. DeKock RL, Schipper LA, Dykhouse SC, Heeringa LP, Brandsen BM (2009) J Chem Edu 86:1459–1464
30. Galabov B, Bobadova-Parvanova P (2000) J Mol Struct 550–551:93–98
31. Miyake T, Aida M (2002) Chem Phys Lett 363:106–110
32. Alkorta I, Blanco F, Deyà PM, Elguero J, Estarellas C, Frontera A, Quiñonero D (2010) Theor Chem Acc 126:1–14
33. Politzer P, Riley KE, Bulat FA, Murray JS (2012) Comput Theor Chem 998:2–8
34. Jose KVJ, Gadre SR (2008) J Chem Phys 128:124310–124319
35. Rincón L, Almeida R, García-Aldea D, y Riega HD (2001) J Chem Phys 114:5552–5561
36. Parra RD, Bulusu S, Zeng XC (2003) J Chem Phys 118:3499–3509
37. Rivelino R, Chaudhuri P, Canuto S (2003) J Chem Phys 118:10593–10601
38. Chen C, Liu M-H, Wu L-S (2003) J Mol Struct (THEOCHEM) 630:187–204
39. Yeole SD, Gadre SR (2011) J Chem Phys 134:084111–084119
40. Araújo RCMU, Soares VM, Oliveira BG, Lopes KC, Ventura E, do Monte SA, Santana OL, Carvalho AB, Ramos MN (2006) Int J Quantum Chem 106:2714–2722
41. Oliveira BG, Araújo RCMU, Soares VM, Ramos MN (2008) J Theor Comput Chem 7:247–256
42. Grabowski SJ, Leszczynski J (2009) Chem Phys 355:169–176
43. Song H-J, Xiao H-M, Dong H-S, Huang Y-G (2006) J Mol Struct (THEOCHEM) 767:67–73
44. Małecka M, Mebs S, Jóźwiak A (2012) Chem Phys 407:20–28
45. Kishi R, Umezaki S-Y, Fukui H, Minami T, Kubota K, Takahashia H, Nakano M (2008) Chem Phys Lett 454:91–96
46. Oliveira BG, Araújo RCMU, Carvalho AB, Ramos MN (2007) Chem Phys Lett 433:390–394
47. Oliveira BG, Araújo RCMU, Carvalho AB, Ramos MN (2009) Struct Chem 20:663–670
48. Desiraju GR (2011) Angew Chem Int Ed 50:52–59
49. Olovsson I (2006) Z Physik Chem 220:963–978
50. Rozas I, Alkorta I, Elguero J (1997) J Phys Chem A 101:9457–9463
51. Domagała M, Grabowski SJ (2009) Chem Phys 363:42–48
52. Oliveira BG, Vasconcellos MLAA, Olinda RR, Filho EBA (2009) Struct Chem 20:81–90
53. Oliveira BG, Araújo RCMU, Ramos MN (2009) J Mol Struct (THEOCHEM) 908:79–83
54. Pejov L, Solimannejad M, Stefov V (2006) Chem Phys 323:259–270
55. Ren F-D, Cao D-L, Wang W-L, Ren J, Hou S-Q, Chen S-S (2009) J Mol Model 15:515–523
56. Nauta K, Miller RE (2001) Chem Phys Lett 346:129–134
57. Araújo RCMU, Silva JBP, Ramos MN (1995) Spectrochim Acta A 51:821–830
58. Araújo RCMU, Ramos MN (1996) J Mol Struct (THEOCHEM) 366:233–240
59. Hanna G, Geva E (2010) Chem Phys 370:201–207
60. Chałasiński G, Szczeüśniak MM (2000) Chem Rev 100:4227–4252
61. Oliveira BG, Araújo RCMU, Pereira FS, Lima EF, Silva WLV, Carvalho AB, Ramos MN (2008) Quim Nova 31:1673–1679
62. Oliveira BG, Araújo RCMU, Ramos MN (2007) Quim Nova 30:1167–1170
63. Oliveira BG, Araújo RCMU, Ramos MN (2010) J Mol Struct (THEOCHEM) 944:168–172
64. van Duijneveldt FB, van Duijneveldt-van de Rijdt JGCM, van Lenthe JH (1994) Chem Rev 94:1873–1885
65. Galano A, Alvarez-Idaboy JR (2006) J Comput Chem 27:1203–1210
66. Boys SF, Bernardi F (1970) Mol Phys 19:553–566
67. Wells BH, Wilson S (1983) Chem Phys Lett 101:429–434
68. Valiron P, Mayer I (1997) Chem Phys Lett 275:46–55
69. Salvador P, Szczęśniak MM (2003) J Chem Phys 118:537–549
70. Hankins D, Moskowitz JW, Stillinger FH (1970) J Chem Phys 53:4544–4554
71. Kotena ZM, Behjatmanesh-Ardakani R, Hashim R, Achari VM (2013) J Mol Model 19:589–599
72. Shields AE, van Mourik T (2007) J Phys Chem A 111:13272–13277
73. Neese F (2009) Coord Chem Rev 253:526–563
74. Drut JE, Furnstahl RJ, Platter L (2010) Prog Part Nuc Phys 64:120–168
75. Li Q, Yin P, Liu Y, Tang AC, Zhang H, Sun Y (2003) Chem Phys Lett 375:470–476
76. Kolboe S, Svelle S (2008) J Phys Chem A 112:6399–6400
77. Altmann JA, Govender MG, Ford TA (2005) Mol Phys 103:949–961
78. Capim SL, Santana SR, Oliveira BG, Rocha GB, Vasconcellos MLAA (2010) J Braz Chem Soc 21:1718–1726
79. Lukin O, Leszczynski J (2002) J Phys Chem A 106:6775–6782
80. Nadim ES, Raissi H, Yoosefian M, Farzad F, Nowroozi AR (2010) J Sulfur Chem 31:275–285
81. Ireta J, Neugebauer J, Scheffler M (2004) J Phys Chem A 108:5692–5698
82. Dkhissi A, Ramaekers R, Houben L, Adamowicz L, Maes G (2000) Chem Phys Lett 331:553–560

83. Pudzianowski AT (1996) J Phys Chem 100:4781–4789
84. Yu W, Liang L, Lin Z, Ling S, Haranczyk M, Gutowski M (2009) J Comput Chem 30:589–600
85. Thürmer S, Seidel R, Winter B (2011) J Phys Chem A 115:6239–6249
86. Csontos J, Palermo NY, Murphy RF, Lovas S (2008) J Comput Chem 29:1344–1352
87. Guadarrama P, Soto-Castro D, Rodríguez-Otero J (2008) Int J Quantum Chem 108:229–237
88. Mayo ML, Gartstein YN (2010) J Chem Phys 132:064503–064510
89. Rao L, Ke H, Fu G, Xu X, Yan Y (2009) J Chem Theory Comput 5:86–96
90. Thanthiriwatte KS, Hohenstein EG, Burns LA, Sherrill CD (2011) J Chem Theory Comput 7:88–96
91. Zhao Y, Truhlar DG (2008) Theor Chem Acc 41:157–167
92. Zhao Y, Tishchenko O, Truhlar DG (2005) J Phys Chem B 109:19046–19051
93. Mandado M, Hermida-Ramón JM (2011) J Chem Theory Comput 7:633–641
94. Bader RFW (1991) Chem Rev 91:893–528
95. Bader RFW (1990) Atoms in molecules. A quantum theory. Oxford University Press, Oxford
96. Mohallem JR (2002) Theor Chem Acc 107:372–374
97. Kryachko ES (2002) Theor Chem Acc 107:375–377
98. Bader RFW (2002) Theor Chem Acc 107:381–382
99. Shahbazian S, Zahedi M (2007) Found Chem 9:85–95
100. Bader RFW, Preston HJT (1969) Int J Quantum Chem 3:327–347
101. Bader RFW (2005) Monatsch Chem 136:819–854
102. Bader RFW (2009) Adv Quantum Chem 57:285–318
103. Bader RFW, Ngyen-Dang TT (1981) Adv Quantum Chem 14:63–124
104. Bader RFW, Anderson SG, Duke AJ (1979) J Am Chem Soc 101:1389–1395
105. Cortés-Guzmán F, Bader RFW (2003) Chem Phys Lett 379:183–192
106. Quiñónez PB, Vila A, Graña AM, Mosquera RA (2003) Chem Phys 287:227–236
107. Solimannejad M, Jamshidi FH, Amani S (2010) J Mol Struct (THEOCHEM) 958:116–121
108. Song H-J, Xiao H-M, Dong H-S, Zhu W-H (2006) J Phys Chem A 110:2225–2230
109. Abdi H, Williams LJ (2010) Principal component analysis. Wiley Interdisciplinary Reviews: Computational Statistics 2:433–459
110. Jolliffe IT (2002) Principal component analysis. Series: Springer series in statistics. Springer, Heidelberg
111. Frisch MJ, Trucks GW, Schlegel HB, Scuseria GE, Robb MA, Cheeseman JR, Zakrzewski VG, Montgomery JA Jr, Stratmann RE, Burant JC, Dapprich S, Millam JM, Daniels AD, Kudin KN, Strain MC, Farkas O, Tomasi J, Barone V, Cossi M, Cammi R, Mennucci B, Pomelli C, Adamo C, Clifford S, Ochterski J, Petersson GA, Ayala PY, Cui Q, Morokuma K, Rega N, Salvador P, Dannenberg JJ, Malick DK, Rabuck AD, Raghavachari K, Foresman JB, Cioslowski J, Ortiz JV, Baboul AG, Stefanov BB, Liu G, Liashenko A, Piskorz P, Komaromi I, Gomperts R, Martin RL, Fox DJ, Keith T, Al-Laham MA, Peng CY, Nanayakkara A, Challacombe M, Gill PMW, Johnson B, Chen W, Wong MW, Andres JL, Gonzalez C, Head-Gordon M, Replogle ES, Pople JA (2001) Gaussian 98, Revision A.11.2. Gaussian, Inc, Pittsburgh
112. Frisch MJ, Trucks GW, Schlegel HB, Scuseria GE, Robb MA, Cheeseman JR, Montgomery JA Jr, Vreven T, Kudin KN, Burant JC, Millam JM, Iyengar SS, Tomasi J, Barone V, Mennucci B, Cossi M, Scalmani G, Rega N, Petersson GA, Nakatsuji H, Hada M, Ehara M, Toyota K, Fukuda R, Hasegawa J, Ishida M, Nakajima T, Honda Y, Kitao O, Nakai H, Klene M, Li X, Knox JE, Hratchian HP, Cross JB, Adamo C, Jaramillo J, Gomperts R, Stratmann RE, Yazyev O, Austin AJ, Cammi R, Pomelli C, Ochterski JW, Ayala PY, Morokuma K, Voth GA, Salvador P, Dannenberg JJ, Zakrzewski VG, Dapprich S, Daniels AD, Strain MC, Farkas O, Malick DK, Rabuck AD, Raghavachari K, Foresman JB, Ortiz JV, Cui Q, Baboul AG, Clifford S, Cioslowski J, Stefanov BB, Liu G, Liashenko A, Piskorz P, Komaromi I, Martin RL, Fox DJ, Keith T, Al-Laham MA, Peng CY, Nanayakkara A, Challacombe M, Gill PMW, Johnson B, Chen W, Wong MW, Gonzalez C, Pople JA (2003) Gaussian 03, Revision B.04. Gaussian, Inc, Pittsburgh
113. The Unscrambler 6.0, Camo Computer-Aided Modeling A/S, Olav Tryggvasonsgt, 24, N-7011 Trondheim, Norway
114. Cioslowski JJ (1989) J Am Chem Soc 111:8333–8336
115. Biegler-König F (2000) AIM 2000 version 1.0. University of Applied Sciences, Bielefeld
116. Keith TA (2011) AIMAll Version 11.05.16. http://aim.tkgristmill.com/
117. Oliveira BG, Leite LFCC (2009) J Mol Struct (THEOCHEM) 915:38–42
118. Hinchliffe A (1983) J Mol Struct (THEOCHEM) 104:421–425
119. Oliveira BG, Vasconcellos MLAA (2009) Struct Chem 20:897–902
120. Lopes KC, Pereira FS, de Araújo RCMU, Ramos MN (2001) J Mol Struct 565–566:417–420
121. Kukolich SG (1983) J Chem Phys 78:4832–4835
122. Li Q, An X, Luan F, Li W, Gong B, Cheng J, Sun J (2008) J Chem Phys 128:154102–154107
123. Joseph J, Jemmis ED (2007) J Am Chem Soc 129:4620–4632
124. Esrafili MD, Behzadi H, Hadipour NL (2008) Theor Chem Acc 123:135–146
125. Freindorf M, Kraka E, Cremer D (2012) Int J Quantum Chem 112:3174–3187
126. Gong B, Jing B, Li Q, Liu Z, Li W, Cheng J, Zheng Q, Sun J (2010) Theor Chem Acc 127:303–309
127. Zabardasti A, Kakanejadi A, Ghenaatian F, Bigleri Z (2010) Mol Simul 36:960–968
128. Zhao Q, Feng D, Hao J (2011) J Mol Model 17:2817–2823
129. Wendler K, Thar J, Zahn S, Kirchner B (2010) J Phys Chem A 114:9529–9536. More details can be found in Fig. 1 of the Suplementary information
130. Grabowski SJ (2012) Comput Theor Chem 992:70–77
131. Grabowski SJ (2007) Chem Phys Lett 436:63–67
132. Hennemann M, Murray JS, Politzer P, Riley KE, Clark T (2012) J Mol Model 18:2461–2469
133. Oliveira BG, Lima MCA, Pitta IR, Galdino SL, Hernandes MZ (2010) J Mol Model 16:119–127
134. Oliveira BG, Ramos MN (2010) Int J Quantum Chem 110:307–316
135. Oliveira BG, Araújo RCMU (2012) J Mol Model 18:2845–2854
136. Flick JC, Kosenkov D, Hohenstein EG, Sherrill CD, Slipchenko LV (2012) J Chem Theory Comput 8:2835–2843
137. Moncada F, Uribe LS, Romero J, Reyes A (2013) Int J Quantum Chem 113:1556–1561
138. McAllister LJ, Bruce DW, Karadakov PB (2012) J Phys Chem A 116:10621–10628
139. da Silva JBP, Neto BB, Ramos MN, Bruns RE (1998) Chemom Intel Lab Sys 44:187–195
140. Araújo RCMU, da Silva JBP, Neto BB, Ramos MN (2002) Chemom Intel Lab Sys 62:37–46
141. Oliveira BG, Araújo RCMU, Carvalho AB, Ramos MN (2009) J Mol Model 15:421–432
142. Oliveira BG, Araújo RCMU, Carvalho AB, Ramos MN (2009) J Mol Model 15:123–131
143. Oliveira BG, Araújo RCMU (2011) Monatsch Chem 142:861–873
144. Oliveira BG, Araújo RCMU (2012) Can J Chem 90:368–375
145. Oliveira BG, Araújo RCMU, Carvalho AB, Ramos MN (2011) J Mol Model 17:2847–2862
146. Cremer D, Kraka E (1985) J Am Chem Soc 107:3800–3810

147. Cremer D, Kraka E (1985) J Am Chem Soc 107:3811–3819
148. Angelina EL, Peruchena NM (2011) J Phys Chem A 115:4701–4710
149. Zhang Y-H, Hao J-K, Wang X, Zhou W, Tang T-H (1998) J Mol Struct (THEOCHEM) 455:85–99
150. Bader RFW (2009) J Phys Chem A 113:10391–10396
151. Matta CF, Boyd RJ (2007) The quantum theory of atoms in molecules. From solid state to DNA and drug design. Wiley-VCH, Weinheim
152. Robertazzi A, Platts JA (2005) Inorg Chem 44:267–274
153. Lewis GN (1916) J Am Chem Soc 38:762–785
154. Pauling L (1935) J Am Chem Soc 57:2680–2684
155. Pimentel GC, McClellan AL (1971) Ann Rev Phys Chem 22:347–385
156. Oliveira BG (2012) Comput Theor Chem 998:173–182
157. Grabowski SJ (2011) Chem Rev 111:2597–2625
158. Grabowski SJ, Sokalski WA, Leszczynski J (2006) J Phys Chem A 110:4772–4779
159. Espinosa E, Alkorta I, Elguero J, Molins E (2002) J Chem Phys 117:5529–5542
160. Oliveira BG (2013) Phys Chem Phys Chem 15:37–79
161. Grabowski SJ (2000) J Mol Struct 553:151–156
162. Wojtulewski S, Grabowski SJ (2002) J Mol Struct 605:235–240
163. Grabowski SJ, Sokalski WA, Leszczynski J (2004) J Phys Chem A 108:5823–5830
164. Lipkowski P, Grabowski SJ, Robinson TL, Leszczynski J (2004) J Phys Chem A 108:10865–10872
165. Grabowski SJ, Sokalski WA, Leszczynski J (2004) J Phys Chem A 108:1806–1812
166. Domagała M, Grabowski SJ (2005) J Phys Chem A 109:5683–5688
167. Raghavendra B, Arunan E (2007) J Phys Chem A 111:9699–9706
168. Cheng M, Pu X, Wong N-B, Li M, Tian A (2008) New J Chem 32:1060–1070
169. Mata I, Alkorta I, Espinosa E, Molins E (2011) Chem Phys Lett 507:185–189
170. Hugas D, Simon S, Duran M (2007) J Phys Chem A 111:4506–4512
171. Grabowski SJ (2001) J Mol Struct 562:137–143
172. Grabowski SJ (2001) Chem Phys Lett 338:361–366
173. Grabowski SJ (2004) J Phys Org Chem 17:18–31
174. Oliveira BG, Pereira FS, de Araújo RCMU, Ramos MN (2006) Chem Phys Lett 427:181–184